Supplementary Information

Wastewater-influenced estuaries are characterized by disproportionately high nitrous oxide emissions but overestimated IPCC emission factor

Yue Dong[1,2], Jia Liu[3,4], Xiang Cheng[1,2,5], Fuqiang Fan[1,2], Wei Lin[1,2], Chunyang Zhou[1,2], Shengrui Wang[1,2,5*], Shangbin Xiao[3,4*], Chenghao Wang[6,7*], Yu Li[1,2], Changlin Li[1,2]

[1] *Guangdong-Hong Kong Joint Laboratory for Water Security, Beijing Normal University, Zhuhai 519087, China*

[2] *Center for Water Research, Advanced Institute of Natural Sciences, Beijing Normal University, Zhuhai 519087, China*

[3]*College of Hydraulic and Environment Engineering, China Three Gorges University, Yichang 443002, China*

[4]*Hubei Field Observation and Scientific Research Stations for Water Ecosystem in Three Gorges Reservoir, China Three Gorges University, Yichang 443002, China*

[5]*College of Water Sciences, Beijing Normal University, Beijing 100875, China*

[6]*School of Meteorology, University of Oklahoma, Norman, OK 73072, USA*

[7]*Department of Geography and Environmental Sustainability, University of Oklahoma, Norman, OK 73019, USA*

[*]Corresponding authors

Emails: wangsr@bnu.edu.cn, shangbinx@163.com, chenghao.wang@ou.edu

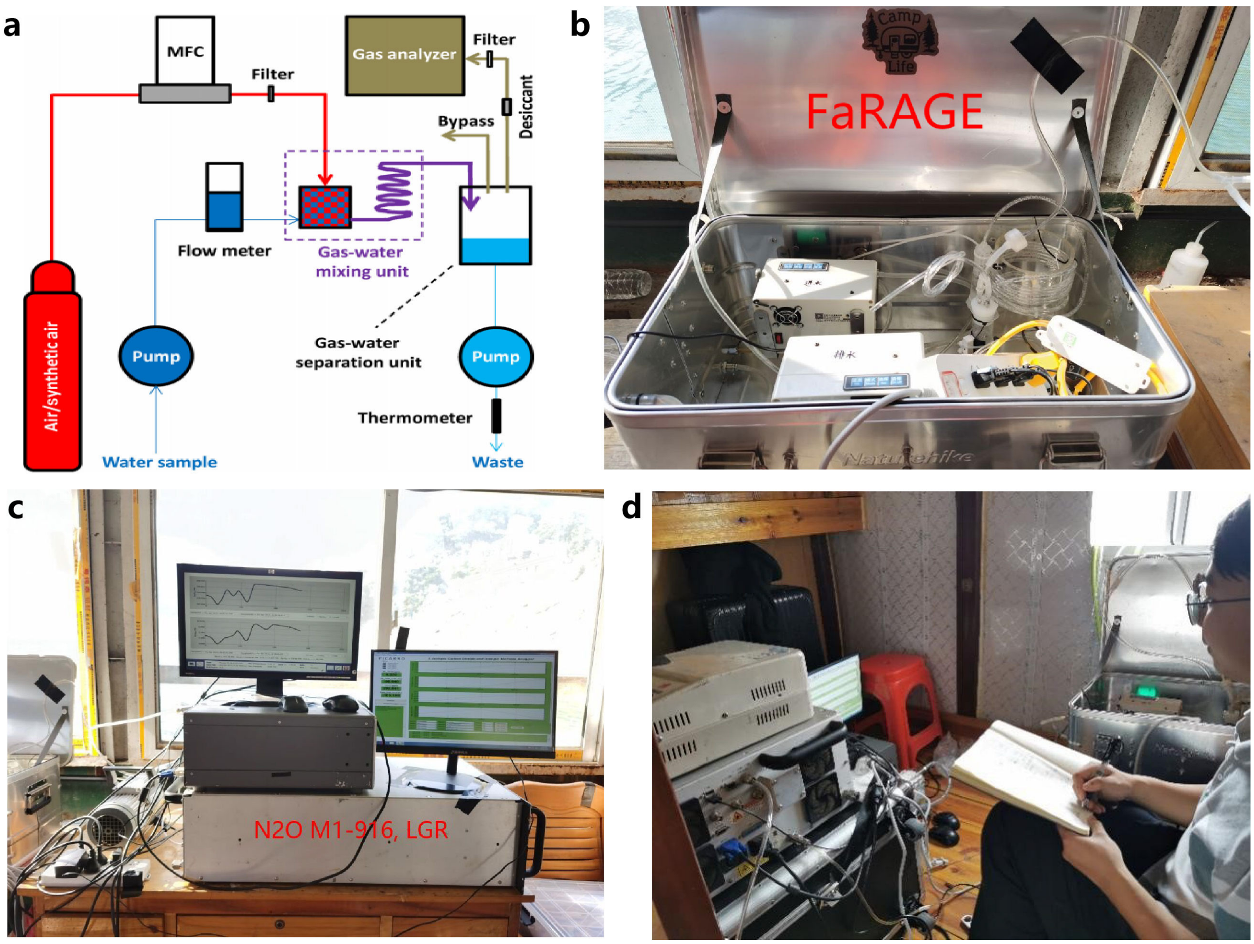

Supplementary Figure 1. High-resolution N_2O monitoring platform used in this study. a, Schematic the FaRAGE system[1]. **b**, Photo of the FaRAGE system used in the field campaign. **c**, The FaRAGE system was coupled with a gas analyzer (N_2O M1-916, LGR). **d**, A researcher monitoring the system.

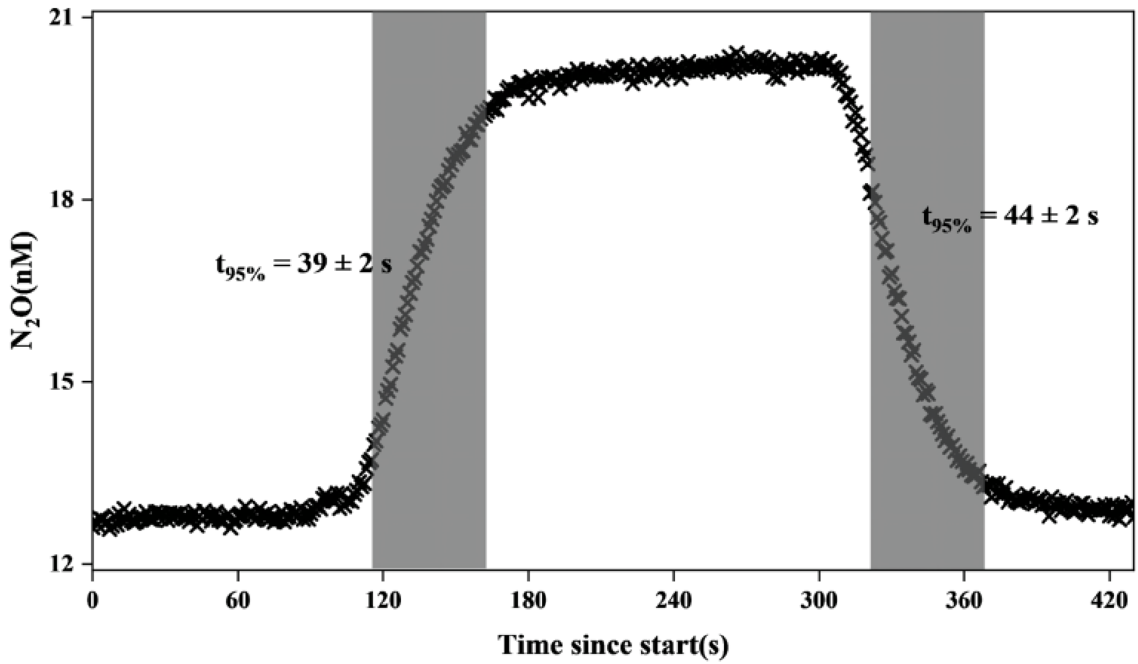

Supplementary Figure 2. Response process of the sample entering into the plateaus of measurement with a response time of 41±2s using the FaRAGE-based N_2O measurements.

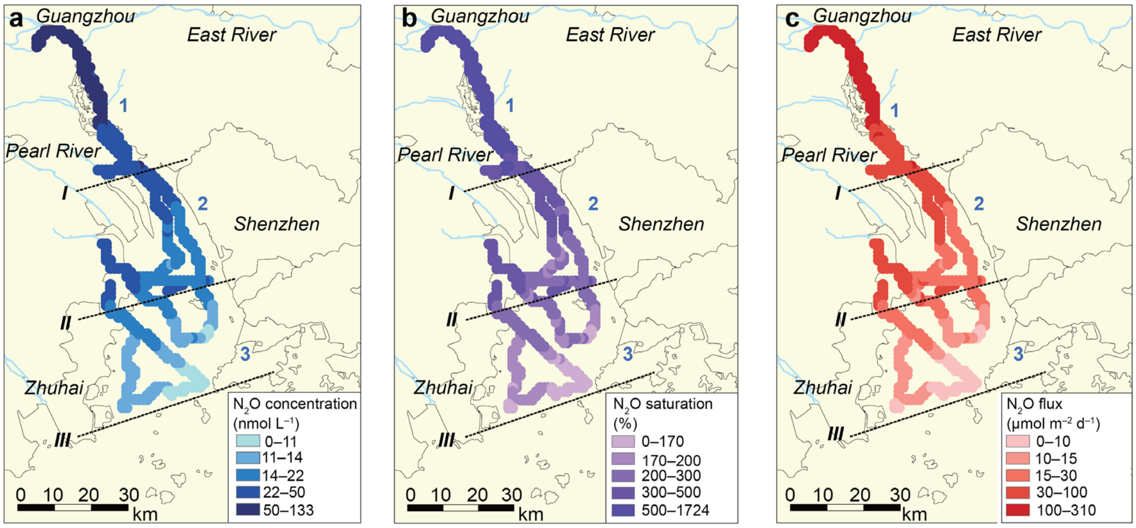

Supplementary Figure 3. Spatial distributions of N_2O concentration, saturation, and flux in PRE from the real-time, high-resolution monitoring. a, Dissolved N_2O concentration. **b**, N_2O saturation. **c**, N_2O flux. The base map is from RESDC data (http://www.resdc.cn/).

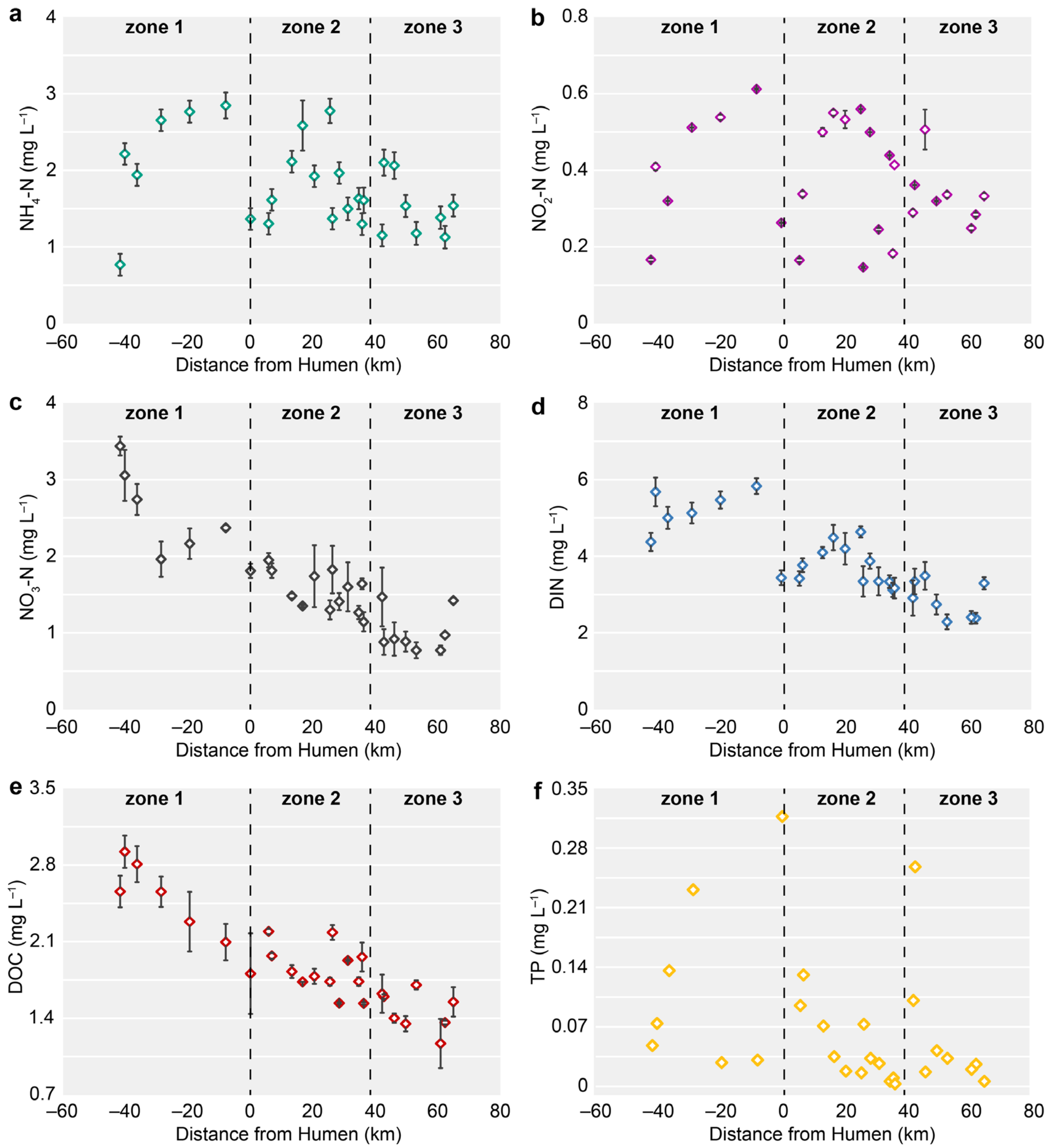

Supplementary Figure 4. Distribution of physicochemical parameters in PRE as a function of distance from Humen. a, NH_4-N. **b**, NO_2-N. **c**, NO_3-N. **d**, DIN. **e**, DOC. **f**, TP**.** The distance is positive downstream of Humen Outlet. Dashed lines in black delineate three zones of PRE: zone 1—upper Estuary (Humen upstream), zone 2—middle Estuary (Inner Lingdingyang), and zone 3—lower Estuary (Outer Lingdingyang).

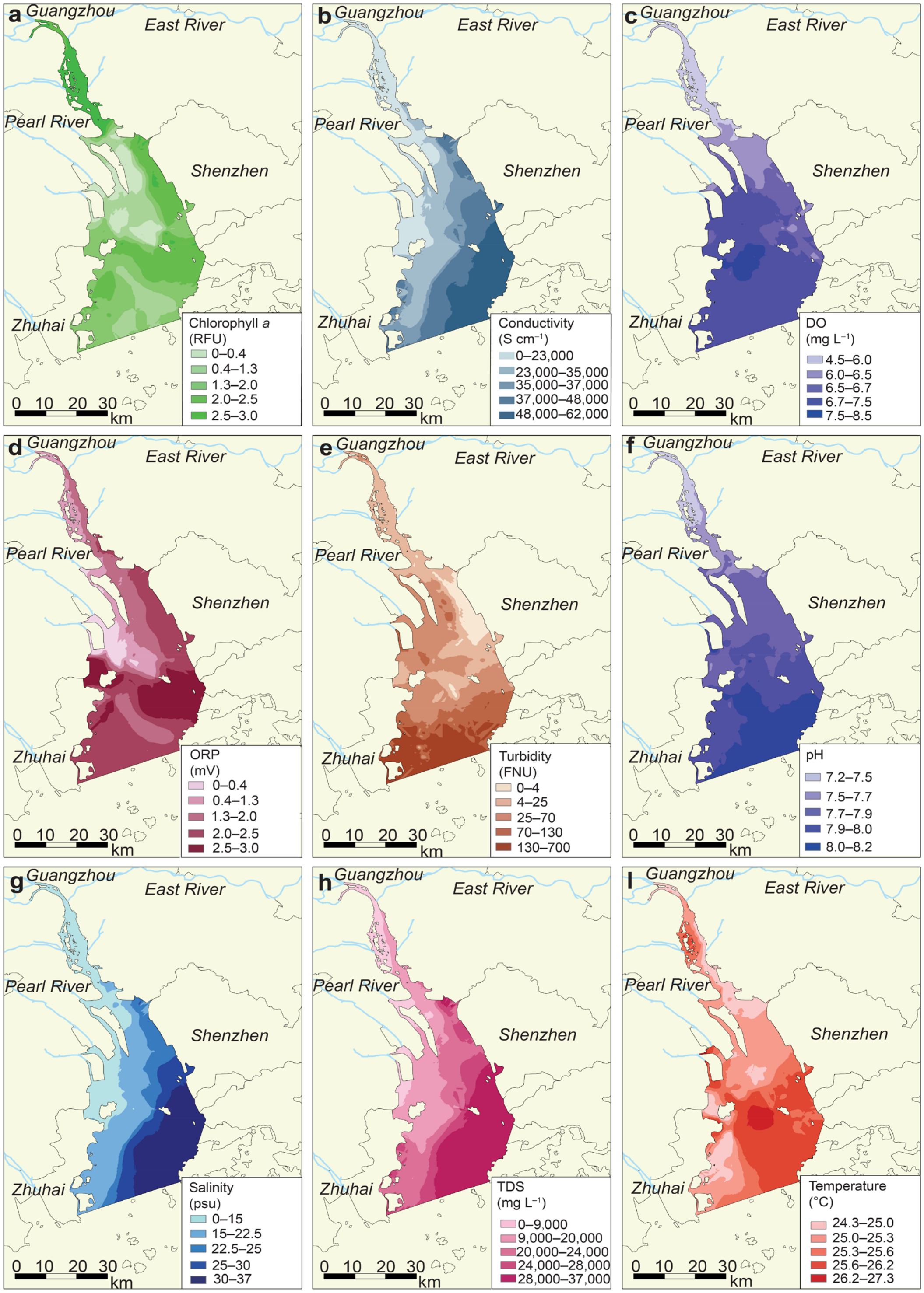

Supplementary Figure 5. Spatial distribution of physicochemical parameters. **a**, Chlorophyll a. **b**, Conductivity. **c**, DO. **d**, ORP. **e**, Turbidity, **f**, pH. **g**, Salinity. **h**, Total dissolved solids (TDS). **i**, Temperature. The base map is from RESDC data (http://www.resdc.cn/).

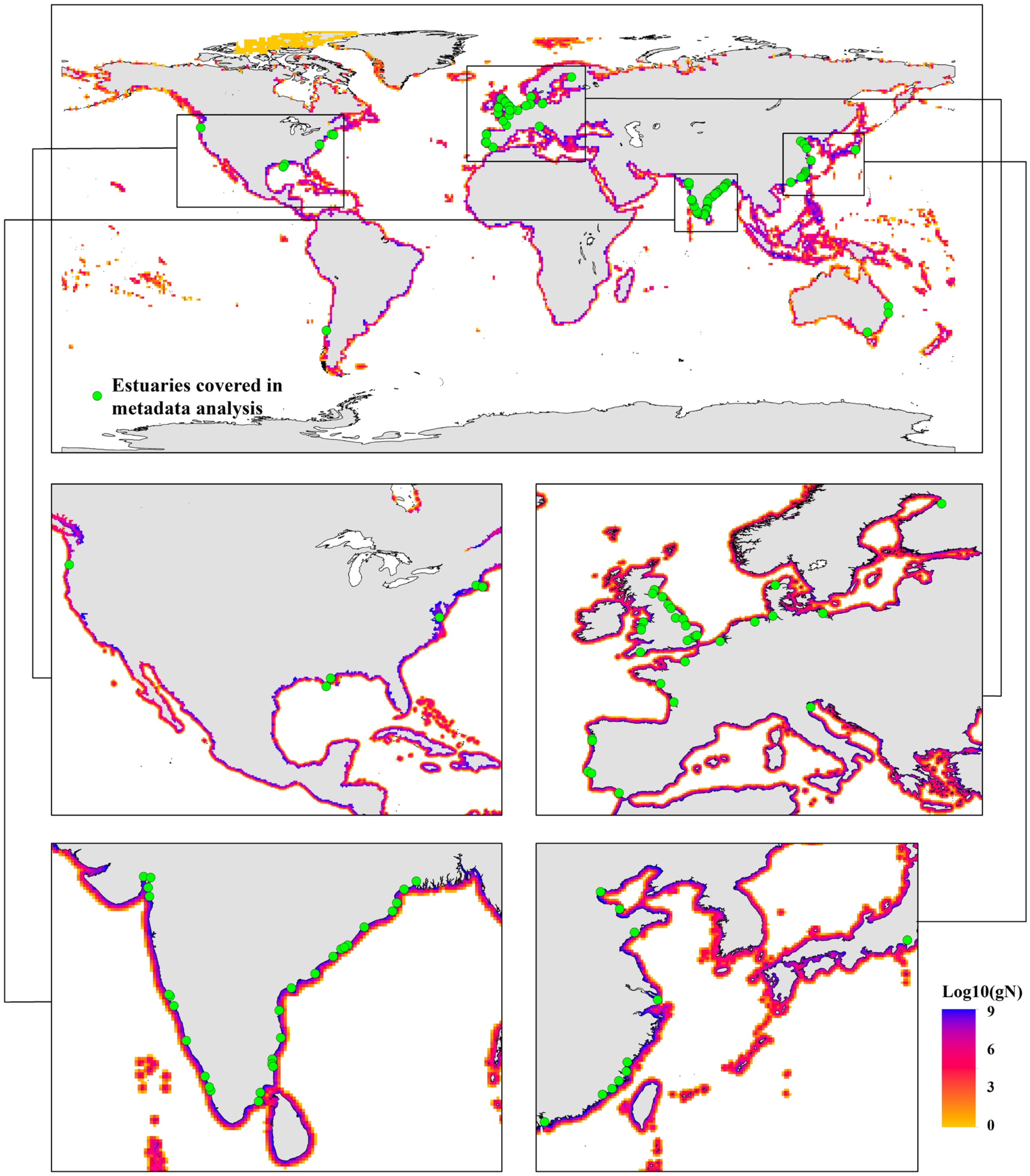

Supplementary Figure 6. The distribution of wastewater nitrogen input and estuarine locations covered in the meta-analysis.

Supplementary Table 1. Goodness of fit for statistics of linear, efficiency loss and Michaelis-Menten model in global, Asian, European, American and Oceania estuaries.

		RSE	Adjusted R^2	p-value	RMSE	AIC
Global	Michaelis–Menten	0.304	0.254	2.547e–41	0.298	32.20
	Linear	0.299	0.274	6.480e–06	0.294	30.50
	Efficiency loss	**0.250**	**0.489**	**1.078e–10**	**0.246**	**8.28**
Asian	**Michaelis–Menten**	**0.269**	**0.281**	**3.367e–19**	**0.258**	**9.43**
	Linear	0.306	0.072	0.100	0.294	16.10
	Efficiency loss	0.277	0.238	0.007	0.266	11.00
European	Michaelis–Menten	0.232	0.423	5.397e–13	0.218	2.46
	Linear	0.256	0.299	0.014	0.240	5.77
	Efficiency loss	**0.233**	**0.419**	**0.003**	**0.219**	**2.57**
American and Oceania	Michaelis–Menten	0.248	0.149	1.216e–10	0.233	4.65
	Linear	**0.1898**	**0.504**	**0.001**	**0.178**	**–4.50**
	Efficiency loss	0.2168	0.351	0.007	0.2038	0.042

Supplementary Table 2. Primer pairs used in qPCR assays and the corresponding amplification conditions.

Gene	Primer	Sequence (5'-3')	Thermal profile	Reaction mixture	Amplification efficiency (%)	Ref.
AOA *amo*A	arch-amoA-23F arch-amoA-616R	ATGGTCTGGCTWAGACG GCCATCCATCTGTATGTCCA	95°C for 3 min, 40 cycles of 5 s at 95°C, 30 s at 58°C, and 1 min at 72°C	10 μL 2X ChamQ SYBR Color qPCR Master Mix, 0.8 μL of each primer (5 μM), 0.4 μL 50 X ROX Reference Dye 1, and 2 μL Template (DNA)	89	1
AOB *amo*A	CTO189f CTO654r	GGAGRAAAGCAGGGGATCG CTAGCYTTGTAGTTTCAAAC GC			105	2
nirS	cd3aF R3cd	GTSAACGTSAAGGARACSGG GASTTCGGRTGSGTCTTGA			104	3
nirK	FlaCu R3cu	ATCATGGTSCTGCCGCG GCCTCGATCAGRTTGTGGTT			101	4
narG	narG-f narG-r	TCGCCSATYCCGGCSATGTC GAGTTGTACCAGTCRGCSGAYTCSG			99	5
nosZ	nosZF nosZR	CGYTGTTCMTCGACAGCCAG CATGTGCAGNGCRTGGCAGAA			96	6

Supplementary References

1. Sahan, E. & Muyzer, G. Diversity and spatio-temporal distribution of ammonia-oxidizing Archaea and Bacteria in sediments of the Westerschelde estuary. *FEMS Microbiol. Ecol.* **64**, 175–186 (2008).
2. Mahmood, S., Freitag, T. E. & Prosser, J. I. Comparison of PCR primer-based strategies for characterization of ammonia oxidizer communities in environmental samples. *FEMS Microbiol. Ecol.* **56**, 482–493 (2006).
3. Zhang, S. *et al.* Linkages between anammox and denitrifying bacterial communities and nitrogen loss rates in high-elevation rivers. *Limnol. Oceanogr.* **66**, 765–778 (2021).
4. Valero, C. *et al.* Nitrification-denitrification in WSP: a mechanism for permanent nitrogen removal in maturation ponds. in *8th IWA Specialist Group Conference on Waste Stabilization Ponds* (2009).
5. Bru, D., Sarr, A. & Philippot, L. Relative abundances of proteobacterial membrane-bound and periplasmic nitrate reductases in selected environments. *Appl. Environ. Microbiol.* **73**, 5971–5974 (2007).
6. Rösch, C., Mergel, A. & Bothe, H. Biodiversity of denitrifying and dinitrogen-fixing bacteria in an acid forest soil. *Appl. Environ. Microbiol.* **68**, 3818–3829 (2002).